

Exploration of Time Reversal for Wireless Communications within Computing Packages

Ama Bandara*
NaNoNetworking Center in
Catalunya (N3Cat)
Universitat Politècnica de Catalunya
Barcelona, Spain
ama.peramuna@upc.edu

Fátima Rodríguez-Galán*
NaNoNetworking Center in
Catalunya (N3Cat)
Universitat Politècnica de Catalunya
Barcelona, Spain
fatima.yolanda.rodriguez@upc.edu

Elana Pereira de Santana
Institute of High Frequency and
Quantum Electronics
University of Siegen
Siegen, Germany
Elana.PSantana@uni-siegen.de

Peter Haring Bolívar
Institute of High Frequency and
Quantum Electronics
University of Siegen
Siegen, Germany
peter.haring@uni-siegen.de

Eduard Alarcón
NaNoNetworking Center in
Catalunya (N3Cat)
Universitat Politècnica de Catalunya
Barcelona, Spain
eduard.alarcon@upc.edu

Sergi Abadal
NaNoNetworking Center in
Catalunya (N3Cat)
Universitat Politècnica de Catalunya
Barcelona, Spain
abadal@ac.upc.edu

ABSTRACT

Wireless Network-on-Chip (WNoC) is a promising paradigm to overcome the versatility and scalability issues of conventional on-chip networks for current processor chips. However, the chip environment suffers from delay spread which leads to intense Inter-Symbol Interference (ISI). This degrades the signal when transmitting and makes it difficult to achieve the desired Bit Error Rate (BER) in this constraint-driven scenario. Time reversal (TR) is a technique that uses the multipath richness of the channel to overcome the undesired effects of the delay spread. As the flip-chip channel is static and can be characterized beforehand, in this paper we propose to apply TR to the wireless in-package channel. We evaluate the effects of this technique in time and space from an electromagnetic point of view. Furthermore, we study the effectiveness of TR in modulated data communications in terms of BER as a function of transmission rate and power. Our results show not only the spatiotemporal focusing effect of TR in a chip that could lead to multiple spatial channels, but also that transmissions using TR outperform, BER-wise, non-TR transmissions it by an order of magnitude.

CCS CONCEPTS

• **Hardware** → **Radio frequency and wireless interconnect**;

KEYWORDS

Wireless-Network-on-Chip; Flip-chip; Time Reversal

1 INTRODUCTION

Modern technological advancements and the end of Moore's Law have driven the field of computer architecture towards heterogeneous Systems-in-Package (SiP), systems hosting an increasing number of CPU, GPU, and specialized accelerator chips [19, 21]. These chips are interconnected through an interposer or a Printed Circuit Board (PCB) and, given the nature of such SiPs, such interconnect needs to support high bandwidth and low latency through multiple parallel signal transmissions within and across the chips.

NoCs and NiP arise to improve the interconnections demands in computing systems [5]. However, conventional wired NoC/NiP approaches suffer from latency and efficiency issues when scaling to a large number of cores/chips and are unable to provide flexibility to manage variable traffic loads or heterogeneous computing technologies [5, 9]. This paved the way for the WNoC paradigm as a potential complement to existing NoCs.

WNoC is a promising technology that takes advantage of electromagnetic (EM) nano-communication [14, 24]. It proposes to have wireless links connecting distant processors across chips and making use of the computing package as propagation medium. The information reaches the destination in a single hop and with latencies of a few nanoseconds irrespective of the communication distance, as opposed to the multi-hop nature of the wired NoCs/NiPs. This allows to relieve or even eliminate the communication bottleneck imposed by the prevailing NoC/NiP communication architectures, promising to accelerate future computing systems [10].

This diminished latency delivered by WNoC comes with a price since wireless bandwidth is limited and needs to be shared among the cores. As a result, Medium Access Control (MAC) protocols and multiplexing schemes are required to avoid collisions and interference [1, 23]. Also, at the physical layer, WNoC needs to adapt to chip resource constraints. The use of mm-wave and terahertz bands allows the integration of tens of antennas within each chip, whereas simple modulations such as On-Off Keying (OOK) are adopted to avoid bulky or power-hungry components at the transceiver [28]. However, with such low order modulations, high symbol rates are needed to reach the 10+ Gb/s speeds expected for WNoC.

The energy propagation around the computing package, which can act as a sort of reverberation chamber, leads to a high delay spread (DS) [6, 11, 22]. This quickly leads to inter-symbol interference (ISI) as we gradually increase the symbol rate to achieve the aforementioned 10+ Gb/s speeds. Therefore, the stringent Bit Error Rate (BER) requirements of this scenario (10^{-15} , similar to the error rate of a wire) are proving difficult to meet [26]. Moreover, in considering multi-node communication with simultaneous signal transmissions as a solution for bandwidth sharing, each node

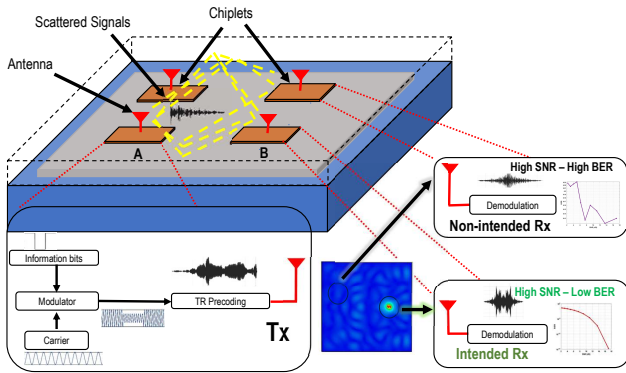


Figure 1: Time reversal in a computing package. Through a filter at the transmitter end, time reversal attains spatiotemporal focusing at an intended receiver, increasing the achievable data rate and opening the door to multiple spatial channels for wireless communications within a computing package.

will be superimposed with another EM wave which could evidently hinder the demodulation of the intended signal and disrupt the communication. It is difficult to claim traditional wireless interference mitigation techniques [25, 29] introduced up to 5G wireless communication protocol stack (unless with modified hybrid architectures) in considering the more realistic signal transmission within the chip to avoid complex transceivers with high power consumption. Hence, a fundamental challenge in WNoC resides in the mitigation of interference and DS effects in reverberating channels towards the creation of multiple parallel high-speed links.

To bridge this gap, this paper proposes the use of Time Reversal in the wireless in-package environment (Figure 1). TR is a technique that employs knowledge of the wireless channel impulse response to create an ideal matched filter [16]. The key of TR is that it can be applied as a filter at the transmitter and, by doing so, the radiated signal is focused in time (with a peak much shorter than the length of the impulse response) and in space (around a targeted receiver). Hence, TR only mitigates potential ISI effects, but also compresses undesirable interference on adjacent transceivers paving the way to having multiple parallel spatial channels.

The benefit of TR in rich scattering environments is well understood and proven. Originally demonstrated in acoustics, TR was then experimentally validated for wireless communications at microwave frequencies [15] and, more recently, sub-terahertz bands [3, 18]. Various modulation schemes have been combined with TR with the aim of transmitting faster than what the DS of the channel would advise [12, 17]. However, since conventional wireless networks typically deal with dynamic channel variations, it is difficult to adopt TR due to the need of constantly obtaining the Channel State Information (CSI) and implementing a filter that can adapt to changes in the CSI.

In this paper, we present a simplified version of TR for WNoC. With the leverage of having prior knowledge of wireless channels within package, which are static, the TR filter(s) can be pre-designed and applied without the need for frequent CSI calculation. To show the proposed approach, we obtain the channel impulse response of a wireless in-package link in CST Microwave Studio and evaluate the spatiotemporal focusing ability of TR in this scenario. We then apply

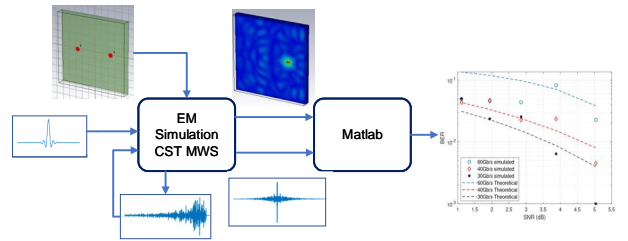


Figure 2: Methodology of this work.

different modulation schemes and analyze the BER as a function of data rate and Signal-to-Noise Ratio (SNR). Compared to a non-TR approach, we show order-of-magnitude improvements for both interference suppression and achievable data rate.

The remainder of this paper is organized as follows. Section 2 offers a characterization of the simulation scenario to be employed in this work. It also contains a detailed description of the TR technique applied to flip-chip package as a tool for interference compression. In Section 3, the spatiotemporal effect of TR in the chip is assessed. Section 4 explores the impact of using TR on the performance of modulated data streams. In Section 6, the paper is concluded.

2 METHODS

Figure 2 summarizes the different methods used in this work. First, we simulate a set of on-chip antennas within a realistic model of a computing package using a full-wave solver, CST Microwave Studio, as described in Sections 2.1 and 2.2. With these simulations, we obtain the impulse response of a particular TX-RX pair. Then, we apply the time-reversal technique as part of the modulation at the transmitter side, as described in Section 2.3.

2.1 Environment Description

We conduct our simulations in an environment that mimics a flip-chip package, widely used in today's processors. In this configuration, the chips are turned over and connected to the system substrate through a set of solder bumps. The packaged chip, therefore, has the silicon substrate on top, which is in turn interfaced by the spreader material and system heat sink on top. The insulator and metal stack are placed at the bottom, interfaced by the solder bumps that connect it to the system [6, 8, 27].

The layers are summarized in Table 1. On top the heat spreader, modeled as Aluminum Nitride, dissipates the heat out of the silicon since it has good thermal conductivity; with $\epsilon_r=8.6$ and $\rho=0.0003$. The insulator is silicon dioxide with $\epsilon_r=3.9$ and $\rho=0.025$. The silicon die is usually made of bulk silicon and serves as the foundation of the transistors. This layer has $\epsilon_r=11.9$ and would normally have a low resistivity ($10 \Omega\text{-cm}$) to favour the operation of digital transistors, yet we consider a high-resistivity silicon layer as in most on-chip antenna works [13, 30] because it dramatically reduces losses at the cost of turning the package in a reverberant environment. In our case, we model this layer as a lossless silicon. Finally, we simulate the interconnects and the bumps as one solid layer of copper [27]. Our chip has a size of $10 \times 10 \text{ mm}^2$ and is to be studied at a frequency of 60 GHz, although the methodology can be reproduced at higher

Table 1: Exploration Parameters.

Parameter	Thickness	Materials	Units
Lateral Spacer	-	Vacuum	N/A
Heat Spreader	0.5	Aluminum Nitride	mm
Silicon die	0.5	High-res. Silicon	mm
Chiplet insulator	0.01	SiO ₂	mm
Bumps	0.0875	Copper	mm

frequencies as well. The channel simulations will be conducted in CST Microwave Studio [7].

2.2 Antenna and Link Characterization

In prior work, the use of a vertical monopole antenna embedded in the silicon layer of the chip has been explored [27]. We model the antenna as a thin metal cylinder that passes vertically through the silicon layer and is fed by the first metal layers. For a 60 GHz frequency, we set the monopole length L to

$$L = \frac{\lambda}{4} = \frac{v_p}{4 \cdot f} = \frac{c_0}{4 \cdot \sqrt{\epsilon_{Si}} \cdot f}. \quad (1)$$

where c_0 is the speed of light, $f = 60$ GHz is the target frequency, and ϵ_{Si} is the permittivity of silicon in that frequency region. Two of the monopole previously described will be placed in the chip at a distance of 7.2 mm from each other. The setup for the simulations, as well as the obtained S parameters, are presented in Figure 3. The S parameters presented are consistent with the presence of high-resistivity silicon, which reduces losses and turns the package into a reverberant environment. This is observed in the resonant nature of the antenna ($S_{11} < -10$ dB at around 60 GHz) and the notchy behavior (but with a moderate average value) of the S_{21} . In comparison, the channel spectra in our prior works with lossy silicon [23] shows a much worse average value without significant notches.

2.3 Time Reversal Formulation

Time reversal is a pulse compression technique which focuses the received signal energy to its source with back propagation, upon creating a signal reversed in time with prior CSI [16]. The technique is suitable for environments with a long impulse response and, hence, a high delay spread. Though we obtain highly correlated channels in close reverberated spaces such as chip environment, by using the exact CIR data correspond to the source, TR is capable of compressing the co-channel interference in a higher extent with transmissions in same time and frequency while taking the multi-path components on the reflections and reverberation to the advantage of energy focusing.

By assuming each node equipped with a wireless communication interface, let us consider a simple wireless signal transmission from node A to node B . Thanks to prior channel characterization, we can assume perfect knowledge of the CIR for such AB link, $h_{AB}(t)$. The time-reversed precoded symbol x_A at node A can be obtained as

$$x_A(t) = h_{AB}(-t) * m_A(t), \quad (2)$$

where $m_A(t)$ are the modulated symbols to be transmitted from node A to node B , $*$ is the convolution operation, and $h_{AB}(-t)$ is

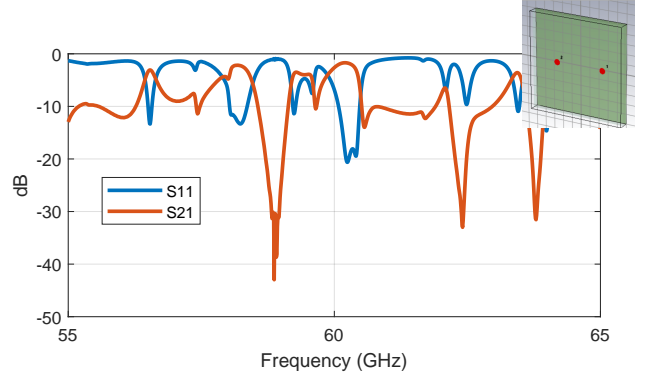


Figure 3: Frequency domain analysis of the proposed antennas and link.

the time-reversed version of the link's CIR, which is

$$h_{AB}(t) = \sum_k \alpha_k e^{j\psi_k} \delta(t - \tau_k), \quad (3)$$

with $\{\alpha_k, \psi_k, \tau_k\}$ being the amplitude, phase and propagation delay of random multi-path component k of the channel $A \rightarrow B$. $\delta(\cdot)$ denotes the Dirac delta function.

The signal coming from node A that would reach a receiver placed in an arbitrary position \vec{r} can be expressed, in the time domain, as

$$\begin{aligned} y(t, \vec{r}) &= h_A(t, \vec{r}) * x_A(t) + n(t) \\ &= h_A(t, \vec{r}) * h_{AB}(-t) * m_A(t) + n(t). \end{aligned} \quad (4)$$

where $h_A(t, \vec{r})$ is the CIR of the channel between the position of A and the arbitrary receiver, while $n(t)$ represents the additive white Gaussian noise (AWGN) at the receiver, assumed of zero mean and variance of σ^2 . For instance, the received signal at node B would be

$$y_B(t) = h_{AB}(t) * h_{AB}(-t) * m_A(t) + n_B(t). \quad (5)$$

As can be observed, Equation (5) is similar to the usual matched filter expression but only happens when $h_A(t, \vec{r}) = h_{AB}(t)$. In other words, the TR transmission creates a spatial matched filter, this is, a matched filter response only when the receiver is placed (i) in B or (ii) in any other position with the same CIR, which could happen due to spatial symmetries.

2.4 Time-Reversal Modulations

As complex transceiver designs are difficult to be incorporated to the WNoC architecture due to high area and power consumption, the basic traditional modulation schemes with simple filters were analysed. In particular, we evaluate Amplitude and Phase Shift Keying (ASK, PSK) and impulse-radio like versions of Pulse Position Modulation (PPM) and On-Off Keying (OOK). The entire analysis is done in MATLAB.

For ASK, the signals were multiplied with a continuous carrier wave by using the amplitude ratio of $A1 : A2 = 0.5$ for the bits $\{0,1\}$, respectively. The BPSK modulation was processed by multiplying the Non-Return to Zero (NRZ) encoded input with a carrier wave. PPM symbols were formed by shifting the impulse radio (IR) on OOK signals with respective prior estimated time shifts.

The data coming from CST was imported in MATLAB and used to create the TR filter as the complex conjugate of $h_{AB}(t)$ and to

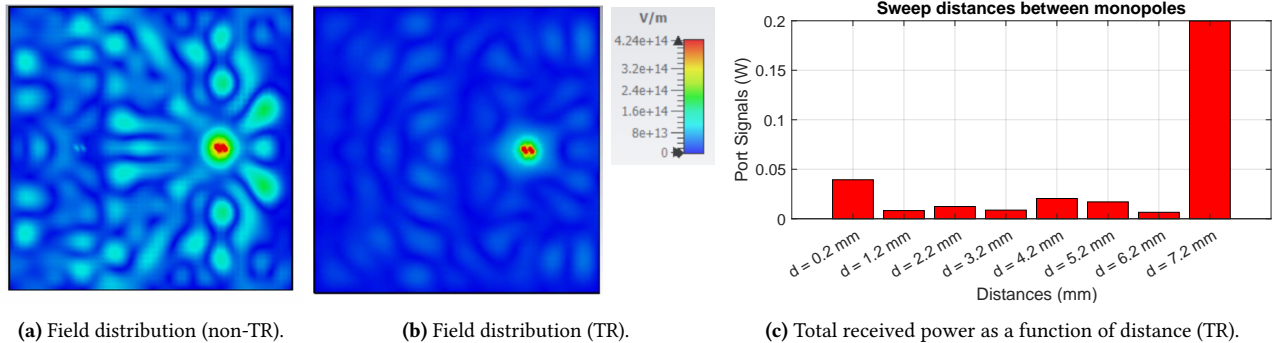


Figure 4: Spatial distribution of energy for non-TR and TR transmissions.

model $h(t, \vec{r})$ in positions of intended and non-intended receivers. The CST data was then convoluted with the modulated data from the synchronised input signals as in Equation (2). Thereafter, the processed TR-modulated symbol was transmitted through the channel(s) as detailed in Equation (4).

The receiver processing was conducted based on the particular modulation employed in the transmitter end such as (i) synchronised carrier multiplication for BPSK prior to the energy detection and, (ii) instantaneous energy detection with a posteriori threshold calculations based on the received signal energy for ASK and PPM. In case of analysing higher order modulation schemes such as M -ary PSK, a similar approach as in BPSK processing can be adopted by multiplying each I and Q phase signal components with the respective synchronised carriers.

3 IMPACT OF TIME REVERSAL ON CHANNEL RESPONSE

In this section, we show the results obtained in the full-wave solver before and after applying time reversal. As described above, the TR process starts by exciting the transmitting antenna at node A with an impulse in the full-wave solver. The channel response is recorded in the time domain at the position of node B , and then time reversed using post-processing. The time-reversed signal is then fed to node A , which radiates it throughout the chip package, but targets node B . Next, we analyze the impact of TR in the spatial response, Section 3.1, and in the temporal response, Section 3.2.

3.1 Spatial Focusing

In order to grasp the impact of TR on the spatial distribution of energy, Figure 4 shows the field distribution for each transmission at the time of higher concentration of energy at the intended receiver. On the one hand, for the non-TR transmission, the energy goes all over the chip, illustrating the reverberant quality of the chip package. Such an effect would cause high ISI and also hinder the creation of concurrent spatial channels. On the other hand, the spatial focusing of the TR transmission is clear, showing a much higher energy level at the targeted location than anywhere else in the chip. Residual energy can be observed in other locations; this is possible if the $h(t)$ between the transmitter location and an arbitrary position is similar to that of the $A \rightarrow B$ link. Yet in our example, the spatial energy scattering is very low compared to the level of spatial focusing achieved by the peak. Hence, we show that

the TR technique manages to compensate our highly reverberant channel.

Additionally, we offer a comparison of the difference in concentration on energy when transmitting with a time reverse $h(t)$ towards a non-desired location. To put this to the test, in the landscape shown in Figure 3, we introduce two monopoles separated by 7.2 mm. This is meant to be our default distance and we calculate and time reversed the $h(t)$ for the link formed when the monopoles are in this default position. Then, keeping the transmitting antenna fixed, we change the position of the receiving antenna, applying a displacement in distance bringing them closer. This will form a different link and therefore a different channel. For each of those, we excite the transmitter with the time reversed $h(t)$ obtained for the default distance.

The results regarding the energy concentration are illustrated in Figure 4c, which shows the total power received in the different positions. In comparison with the default distance of 7.2 mm, the power received in other distances is very low, meaning that the position of the antenna in the chip will influence the channel response. This proves that we can have a transmission in the intended destination with a high concentration of energy that can be ignored in other spots that are of no interest for the transmission. This is an important conclusion because to have the spatiotemporal focusing that comes with TR we need to use the specific $h(t)$ inherent to each link, giving us the opportunity to have simultaneous transmissions of point-to-point for different links with good concentration and little interference.

3.2 Temporal Focusing

Figure 5 shows a comparison of the signal received in antenna 2 without using TR and when we applied it. For a fair comparison, the *time-reversal filter* is normalized so that the radiated power at antenna 1 is the same in both cases. From this figure, we can first observe that the amplitude of the focusing peak is much higher, around three orders of magnitude, than the that of the non-TR signal. It is also clear that the energy is concentrated and not spread over time.

Finally, to illustrate jointly the spatiotemporal effect of TR, we evaluate the received signal over time both in our targeted antenna 2 and in another antenna placed in an arbitrary close location. As Figure 6 shows, the peak is clearly visible in the target antenna,

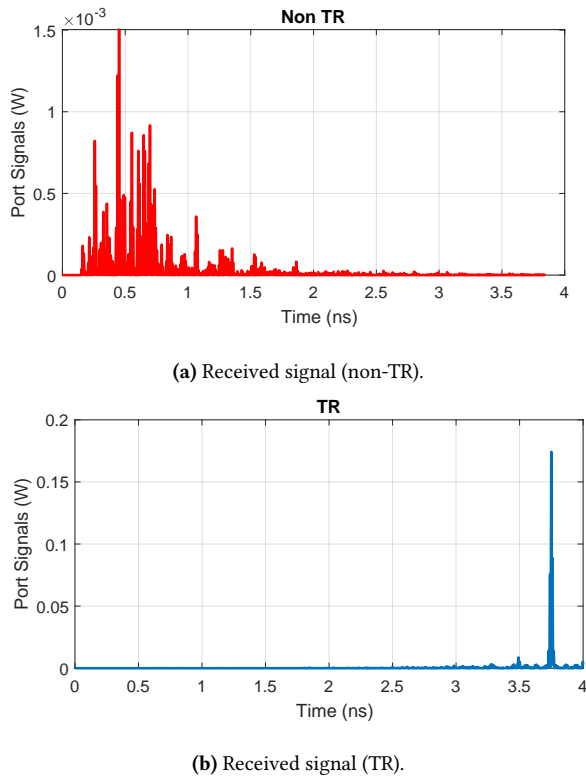


Figure 5: Temporal energy distribution for non-TR and TR transmissions.

whereas a level around an order of magnitude lower is received in the other nearby antennas.

The effect of less interference on nearby nodes paves the way toward parallel transmissions on the chip environment, by sharing same frequency/time resources and a different *time-reversal channel*. Though the channels could be highly correlated within the reverberant chamber, the rich scattered EM distribution of the received signal compresses the interference to an acceptable amount, unless the nodes are placed significantly closer to each other.

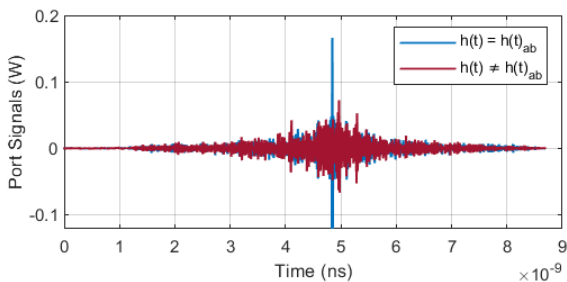


Figure 6: Spatiotemporal focusing: received signal at the intended and non-intended antennas.

4 IMPACT OF TIME REVERSAL ON COMMUNICATION PERFORMANCE

With the superior spatiotemporal focusing observed with a full-wave solver, it is worthwhile to explore the impact on the communications performance. With the extended delay spread due to reverberation as observed in Figure 5a, it is difficult to fit modulated signal transmission as the received signal is disrupted in high-rate transmissions due to ISI. Thus as mentioned in Section 2.4, TR-modulated signal transmissions were analysed to access the performance, importing the $h(t)$ from the full-wave solver.

4.1 Rate Analysis

The BER of obtained for PSK, ASK, PPM for both impulse radio (IR) and continuous wave (CW) transmissions with 16dB constant SNR and increasing rates can be observed in Figure 7(a)-(c).

It is shown that, at constant SNR, ASK attains a superior performance with TR by reaching 60 Gb/s with approximately zero BER (limited by the number of simulated bits), while for the non-TR transmissions the performance sharply decreases beyond 5Gb/s. For PSK, a mediocre performance is observed in compared with ASK, but compared with non-TR transmissions, the ISI is at a very low rate for until the data rate reaches 20 Gb/s. PPM and IR-OOK is with equal acceptable performance rates with TR though in PPM multi-node data multiplexing modulation scheme could be introduced in time/frequency with carefully designed additional time shifts for each node. Although not shown for the sake of brevity, it was observed that approximately around 1-5 Gb/s data rates, higher-order modulations such as QPSK/8-PSK has also shown promising results with TR processing.

4.2 Power Analysis

The BER performance of ASK and PPM is further analysed with SNR by maintaining fixing the noise power and increasing the transmitted power. As the simulation measurements were limited with the time consumption on single round cycle detection on higher SNR values, a theoretical BER expression was derived for ASK and PPM bit detection with respect to amplitude shift of scattered received bits. The centroid of the each received bit cluster with 1000 bits was measured and the shift of amplitude (ΔA) was computed. By assuming equiprobable symbols $\{0, 1\}$, then

$$BER_{theoretical} = \frac{1}{2}Q\left(\frac{\Delta A}{\sigma}\right) \quad (6)$$

with σ being the standard deviation of AWGN and $Q(\cdot)$ being the Q-function. The formulation above was used with the measured amplitude shifts to explore the BER values below 10^{-3} to examine whether the performance with modulations would be compatible with the stringent BER requirements of WNoC.

As shown in Figure 7, even with the presence of noise, ASK performed very well with 10 Gb/s bandwidth having 10^{-15} BER at 17dB. While not shown in the figure, at 60 Gb/s the BER value increases to around 0.02 for ASK. Though the BER performance of PPM was not as well as ASK, an acceptable decrement of values, approximately 10^{-5} in 17dB can be observed in Figure 7, which could positively lead to lower BER values with increment of signal

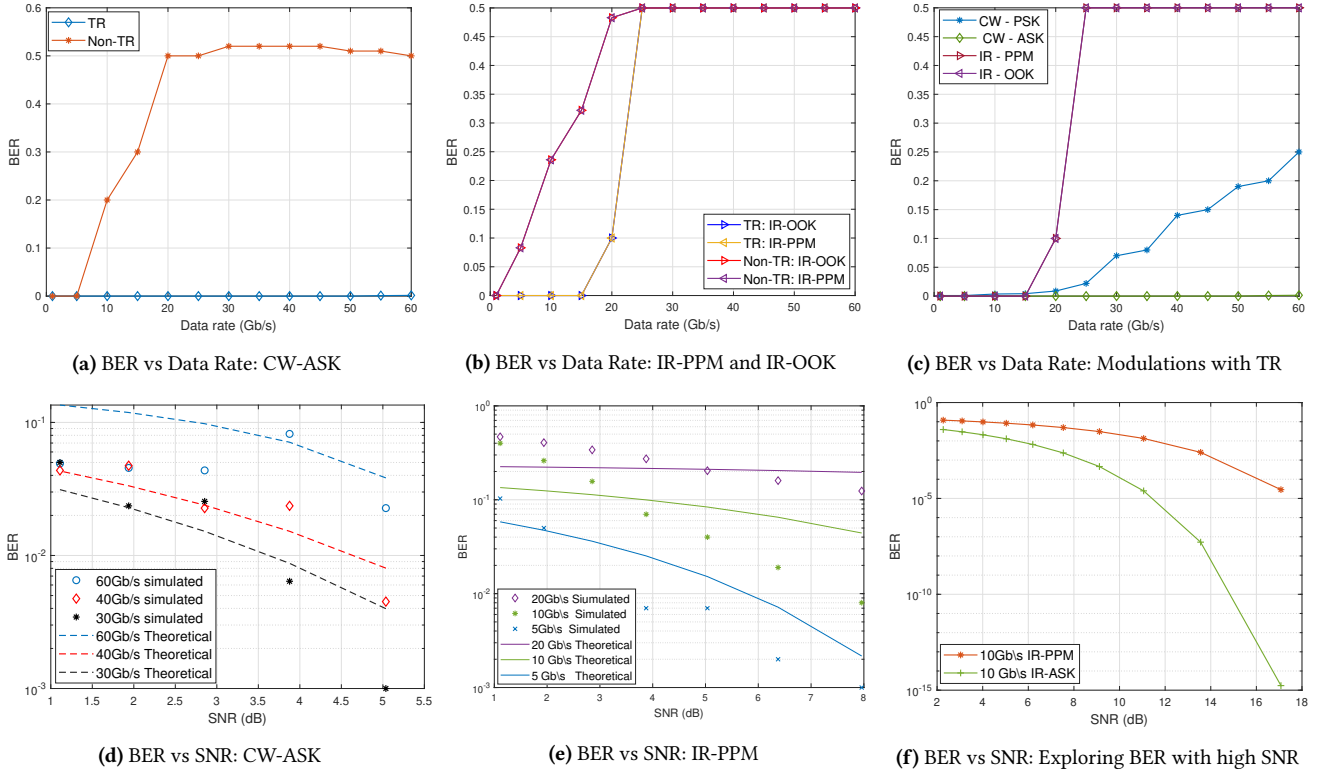


Figure 7: Performance of TR with modulations. Unless noted, the SNR is 16 dB and data rate is 10 Gb/s.

power. As increasing data rates place the bits closer upon reception, it is hard to adopt PPM beyond 15Gb/s. Furthermore, it was observed with simulations an early BER saturation with a lower performance for PSK comparatively with other modulations. Therefore, the theoretical analysis was limited to ASK and PPM.

5 RELATED WORK

Time Reversal in Other Environments. Time reversal is a technique that has been researched in a variety of domains, especially in acoustics [15]. The possibility of transposing the idea of TR to wireless communications is also discussed and proven at microwave frequencies in [16]. They argue that a TR antenna will compensate for the multipath that comes with the large-scale wireless channel and also be able to increase the transmission rate as a result of the reverberation of the medium. There has been also research on applied TR at very high frequencies. In [18], the authors propose to exploit the diversity of the channel and assess the performance of TR technique at a carrier frequency of 273 GHz. Their multipath channel for this approach was created using an aluminum tube as waveguide. An extension of this work is presented in [3], which shows spatiotemporal focusing in three different scenarios also including subTHz bands. Besides the previous examples, some experimental studies [12, 17] have also explored the combination of the TR technique with multiple modulations. The main difference of our work with respect to the previous examples resides in the environment, which is a chip package instead of larger setups emulating indoor environments, for instance. Another difference is the use of the non-static conventional version of TR, where a two-way

approach is required, i.e. frequent probing to obtain the CIR and then the actual application of TR. Instead, we can take advantage of the quasi-deterministic and time-invariant channel to pre-calculate the CIR only once.

Arrays and Spatial Multiplexing. An alternative to TR to increase the capacity of the wireless network is to use arrays to obtain spatial channels through highly directive transmissions. In the context of chip-scale communications, beam forming and beam switching have been studied in multiple works. In [4, 20], authors use planar arrays at 60 GHz. In [2], authors take advantage of the proximity of antennas in multiple processors of the chip and exploit the existing infrastructure to form antenna arrays in a dynamic and opportunistic fashion. More recently, in [23], a compact phased array is proposed to achieve concurrent multicast channels at 60 GHz and 110 GHz. All these works, however, consider either unpackaged configurations (i.e. open-die) [4, 20] or flip-chip with lossy silicon [2, 23], in which cases the DS is limited. However, processors are typically fully packaged as we consider in this work, which either limits the efficiency due to losses or the speed due to DS. Here, we achieve both speed and efficiency thanks to TR.

6 CONCLUSION

In this study, we analysed the performance of WNoC with a simplified version of time-reversal signal transmission on a flip-chip package. Initial experiments were conducted to evaluate the spatiotemporal focusing effect with a full-wave solver. Then, we combined time-reversal with simple modulations at high frequencies and analyzed its performance. It was demonstrated that with ASK/PSK/PPM

pre-coded with time reversal provides acceptable bit error rates beyond 10 Gb/s. ASK provided the best BER performance with 10^{-15} at 10 Gb/s in 17dB AWGN, by complying with the stringent BER requirements of the scenario. Furthermore, the interference compression exhibited with TR upon transmitting signals suggests that parallel concurrent signal transmissions can be achieved within the same time/frequency channel with minimum interference. In future work, we aim to explore such multiplexing capabilities as well as the impact of non-ideal filters on the performance of the TR technique.

ACKNOWLEDGMENT

Authors acknowledge support from the European Union's Horizon 2020 research and innovation program, grant agreement 863337 (WiPLASH), as well as the European Research Council (ERC) under grant agreement 101042080 (WINC).

REFERENCES

- [1] Sergi Abadal, Robert Guirado, Hamidreza Taghvaei, Akshay Jain, Elana Pereira de Santana, Peter Haring Bolivar, Mohamed Saeed, Renato Negra, Zhenxing Wang, Kun-Ta Wang, et al. 2022. Graphene-based wireless agile interconnects for massive heterogeneous multi-chip processors. *IEEE Wireless Communications* (2022).
- [2] Sergi Abadal, Adrián Marruedo, Antonio Franques, Hamidreza Taghvaei, Albert Cabellos-Aparicio, Jin Zhou, Josep Torrellas, and Eduard Alarcón. 2019. Opportunistic Beamforming in Wireless Network-on-Chip. In *2019 IEEE International Symposium on Circuits and Systems (ISCAS)*. 1–5.
- [3] George C. Alexandropoulos, Ali Mokh, Ramin Khayatizadeh, Julien de Rosny, Mohamed Kamoun, Abdelwaheb Ourir, Arnaud Tourin, Mathias Fink, and Mérouane Debbah. 2022. Time Reversal for 6G Spatiotemporal Focusing: Recent Experiments, Opportunities, and Challenges. *IEEE Vehicular Technology Magazine* 17, 4 (2022), 74–82. <https://doi.org/10.1109/MVT.2022.3196481>
- [4] Prabhat Baniya, Aimeric Bisognin, Kathleen L. Melde, and Cyril Luxey. 2018. Chip-to-Chip Switched Beam 60 GHz Circular Patch Planar Antenna Array and Pattern Considerations. *IEEE Transactions on Antennas and Propagation* 66, 4 (2018), 1776–1787.
- [5] Davide Bertozzi, Giorgos Dimitrakopoulos, José Flich, and Sören Sonntag. 2015. The fast evolving landscape of on-chip communication. *Design Automation for Embedded Systems* 19, 1 (2015), 59–76.
- [6] Yi Chen and Chong Han. 2019. Channel modeling and characterization for wireless networks-on-chip communications in the millimeter wave and terahertz bands. *IEEE Transactions on Molecular, Biological and Multi-Scale Communications* 5, 1 (2019), 30–43.
- [7] Computer Simulation Technology (CST). 2022. CST Microwave Studio. (2022). <http://www.cst.com>
- [8] Ihsan El Masri, Thierry Le Gougec, Pierre-Marie Martin, Rozenn Allanic, and Cedric Quendo. 2019. Electromagnetic Characterization of the Intra-chip Propagation Channel in Ka and V Bands. *IEEE Transactions on Components, Packaging and Manufacturing Technology* 9, 10 (2019), 1931–1941. <https://ieeexplore.ieee.org/document/8768409/>
- [9] Amlan Ganguly, Sergi Abadal, Ishan Thakkar, Natalie Enright Jerger, Marc Riedel, Masoud Babaie, Rajeev Balasubramanian, Abu Sebastian, Sudeep Pasricha, and Baris Taskin. 2022. Interconnects for DNA, Quantum, In-Memory, and Optical Computing: Insights From a Panel Discussion. *IEEE micro* 42, 3 (2022), 40–49.
- [10] Robert Guirado, Hyoukjun Kwon, Sergi Abadal, Eduard Alarcón, and Tushar Krishna. 2021. Dataflow-architecture co-design for 2.5 D DNN accelerators using wireless network-on-package. In *2021 26th Asia and South Pacific Design Automation Conference (ASP-DAC)*. IEEE, 806–812.
- [11] Mohammadreza F Imani, Sergi Abadal, and Philipp del Hougne. 2022. Metasurface-Programmable Wireless Network-on-Chip. *Advanced Science* (2022).
- [12] Yuanwei Jin, Yujie Ying, and Deshuang Zhao. 2011. Time Reversal Data Communications on Pipes Using Guided Elastic Waves - Part II: Experimental Studies. *Proceedings of SPIE - The International Society for Optical Engineering* (03 2011). <https://doi.org/10.1117/12.880273>
- [13] Namhoon Kim, Daniel Wu, Dongwook Kim, Arif Rahman, and Paul Wu. 2011. Interposer design optimization for high frequency signal transmission in passive and active interposer using through silicon via (TSV). In *2011 IEEE 61st electronic components and technology conference (ECTC)*. Ieee, 1160–1167.
- [14] Avinash K Kodi, Ashif I Sikder, Dominic Ditomaso, Savas Kaya, David Matolak, and William Rayess. 2015. Kilo-core Wireless Network-on-Chips (NoCs) Architectures. In *Proceedings of the NANOCOM '15*. Art. 33.
- [15] Geoffroy Lerosey, J De Rosny, A Tourin, A Derode, G Montaldo, and M Fink. 2004. Time reversal of electromagnetic waves. *Physical review letters* 92, 19 (2004), 193904.
- [16] Geoffroy Lerosey, J De Rosny, A Tourin, A Derode, G Montaldo, and M Fink. 2005. Time reversal of electromagnetic waves and telecommunication. *Radio science* 40, 06 (2005), 1–10.
- [17] Shengxing Liu, Zhenhua Zhao, Rouchi Chen, and Wenlong Wu. 2021. Time reversal pulse position modulation communication in shallow water acoustic channels. *Applied Acoustics* 182 (2021), 108249. <https://doi.org/10.1016/j.apacoust.2021.108249>
- [18] Ali Mokh, Julien de Rosny, George C Alexandropoulos, Mohamed Kamoun, Abdelwaheb Ourir, Ramin Khayatizadeh, Arnaud Tourin, and Mathias Fink. 2022. Experimental validation of time reversal multiple access for UWB wireless communications centered at the 273 GHz frequency. In *2022 IEEE 95th Vehicular Technology Conference (VTC2022-Spring)*. IEEE, 1–5.
- [19] Samuel Naffziger, Noah Beck, Thomas Burd, Kevin Lepak, Gabriel H Loh, Mahesh Subramony, and Sean White. 2021. Pioneering chiplet technology and design for the amd epyc™ and ryzen™ processor families: Industrial product. In *2021 ACM/IEEE 48th Annual International Symposium on Computer Architecture (ISCA)*. IEEE, 57–70.
- [20] Rounak Singh Narde, Jayanti Venkataraman, Amlan Ganguly, and Ivan Puchades. 2020. Antenna Arrays as Millimeter-Wave Wireless Interconnects in Multichip Systems. *IEEE Antennas and Wireless Propagation Letters* 19, 11 (2020), 1973–1977.
- [21] Robert M. Radway, Andrew Bartolo, Paul C. Jolly, Zainab F. Khan, Binh Q. Le, Pulkit Tandon, Tony F. Wu, Yunfeng Xin, Elisa Vianello, Pascal Vivet, Etienne Nowak, H. S.Philip Wong, Mohamed M.Sabry Aly, Edith Beigne, Mary Wootters, and Subhashish Mitra. 2021. Illusion of large on-chip memory by networked computing chips for neural network inference. *Nature Electronics* 4, 1 (2021), 71–80. <https://doi.org/10.1038/s41928-020-00515-3>
- [22] William Rayess, David W. Matolak, Savas Kaya, and Avinash Karanth Kodi. 2017. Antennas and Channel Characteristics for Wireless Networks on Chips. *Wireless Personal Communications* 95, 4 (2017), 5039–5056. <https://doi.org/10.1007/s11277-017-4144-0>
- [23] Fátima Rodríguez-Galán, Elana Pereira de Santana, Peter Haring Bolivar, Sergi Abadal, and Eduard Alarcón. 2022. Towards spatial multiplexing in wireless networks within computing packages. In *Proceedings of the 9th ACM International Conference on Nanoscale Computing and Communication*. 1–6.
- [24] Shahriar Shamim, Naseef Mansoor, Rounak Singh Narde, Vignesh Kothandapani, Amlan Ganguly, and Jayanti Venkataraman. 2017. A Wireless Interconnection Framework for Seamless Inter and Intra-chip Communication in Multichip Systems. *IEEE Trans. Comput.* 66, 3 (2017), 389–402. <https://doi.org/10.1109/TC.2016.2605093>
- [25] G.L. Stuber, J.R. Barry, S.W. McLaughlin, Ye Li, M.A. Ingram, and T.G. Pratt. 2004. Broadband MIMO-OFDM wireless communications. *Proc. IEEE* 92, 2 (Feb 2004), 271–294. <https://doi.org/10.1109/JPROC.2003.821912>
- [26] Xavier Timoneda, Sergi Abadal, Antonio Franques, Dionysios Manassis, Jin Zhou, Josep Torrellas, Eduard Alarcón, and Albert Cabellos-Aparicio. 2020. Engineer the channel and adapt to it: Enabling wireless intra-chip communication. *IEEE Transactions on Communications* 68, 5 (2020), 3247–3258.
- [27] Xavier Timoneda, Albert Cabellos-Aparicio, Dionysios Manassis, Eduard Alarcón, and Sergi Abadal. 2018. Channel characterization for chip-scale wireless communications within computing packages. In *2018 Twelfth IEEE/ACM International Symposium on Networks-on-Chip (NOCS)*. IEEE, 1–8.
- [28] Changhwan Yi, Dongkyo Kim, Sourabh Solanki, Jae Hong Kwon, Moonil Kim, Sanggeun Jeon, Young Chai Ko, and Inkyu Lee. 2021. Design and Performance Analysis of THz Wireless Communication Systems for Chip-to-Chip and Personal Area Networks Applications. *IEEE Journal on Selected Areas in Communications* 39, 6 (2021), 1785–1796. <https://doi.org/10.1109/JSAC.2021.3071849>
- [29] H. Yu, H.D. Tuan, A.A. Nasir, M. Debbah, and Y. Fang. 2022. New generalized zero forcing beamforming for serving more users in energy-harvesting enabled networks. *Physical Communication* 50 (2022), 101500. <https://doi.org/10.1016/j.phycom.2021.101500>
- [30] Yue Ping Zhang, Zhi Ming Chen, and Mei Sun. 2007. Propagation mechanisms of radio waves over intra-chip channels with integrated antennas: Frequency-domain measurements and time-domain analysis. *IEEE Transactions on Antennas and Propagation* 55, 10 (2007), 2900–2906.